



1

1

2

3 Technical note: Large offsets between different datasets of sea water isotopic
4 composition:

5 an illustration of the need to reinforce intercalibration efforts

6

7

8 Gilles Reverdin¹, Claire Waelbroeck¹, Antje H. L. Voelker^{2,3}, Hanno Meyer⁴

9

10

11

12 ¹ LOCEAN, SU/CNRS/IRD/MNHN, Paris, France

13 ² IPMA, Alges, Portugal

14 ³ CCMAR, Faro, Portugal

15 ⁴ AWI Potsdam, Potsdam, Germany

16

17 Corresponding author: Gilles Reverdin gilles.reverdin@locean.ipsl.fr

18



2

19 Abstract

20 We illustrate offsets in seawater isotopic composition between the data sets presented in two
21 recent studies and the LOCEAN seawater isotopic composition dataset, as well as other data
22 for the same years and same regions. These comparisons are carried in the surface waters, for
23 one in the North and South Atlantic, and for the other in the subtropical South-East Indian
24 Ocean. The observed offsets between data sets which exceed 0.10‰ in $\delta^{18}\text{O}$ and 0.50‰ in
25 $\delta^2\text{H}$ might in part reflect seasonal or spatial variability. However, they are rather systematic,
26 so they likely originate, at least partially, from different instrumentations and protocols used
27 to measure the water samples. They need to be adjusted in order to ultimately merge the
28 different data sets. This highlights the need to actively share seawater isotopic composition
29 samples dedicated to specific intercomparison of data produced in the different laboratories.

30



3

31

32 1. Introduction

33 Seawater isotopic composition ($^{18}\text{O}/^{16}\text{O}$ and $^2\text{H}/^1\text{H}$ ratios expressed as $\delta^{18}\text{O}$ and $\delta^2\text{H}$ in
34 ‰ in the VSMOW/SLAP scale) is classified as an Essential Ocean/Climate Variable
35 (EOV/ECV) in international programs such as GEOTRACES and GO-SHIP. Stable
36 seawater isotopes ($\delta^{18}\text{O}$, $\delta^2\text{H}$) are used to trace sources of freshwater (precipitation,
37 evaporation, runoff, melting glaciers, sea ice formation and melting), both at the ocean
38 surface and in the ocean interior (Schmidt et al., 2007; Hilaire-Marcel et al., 2021).
39 Except for fractionation during phase changes, the water isotopic composition is nearly
40 conservative in the ocean. A major emphasis is on high latitude oceanography, where
41 continental (or iceberg) glacial melt, formation or melt of sea ice, and high-latitude river
42 inputs (for the Arctic) leave different imprints on the surface ocean isotopic
43 composition. In contrast, few studies have been performed on the isotopic signature in
44 the deep ocean (e.g., Prasanna et al., 2015; Voelker et al., 2015). Seawater isotopes in the
45 upper ocean at low latitudes are often vital for paleoclimatic studies, as they are needed
46 to calibrate proxies of past ocean variability in marine carbonate records such as corals
47 and foraminifera (e.g., PAGES CoralHydro2k working group; Konecky et al., 2020).
48 Seawater isotopes are also important tracers in the coastal ocean, with emphasis on
49 upwelling (Conroy et al., 2014, 2017; Kubota et al., 2022; Lao et al., 2022), and river
50 discharges (e.g., Amazon) (Karr and Showers, 2001). Surface ocean seawater isotopes
51 are also used to characterize evaporation rates and air-sea interactions (Benetti et al.,
52 2017). The isotopic signatures of these different processes are evolving in our warming
53 world, which will imprint on the seawater isotopic composition (Oppo et al., 2007).
54 Additionally, seawater isotope data provide model boundary conditions and allow the
55 assessment of model performance in isotope-enabled Earth system models (e.g. Schmidt
56 et al., 2007; Brady et al., 2019; Cauquoin et al., 2019), thereby improving climate model
57 projections of the future.

58 Stable seawater isotope data have thus been massively produced in the last decades by
59 a variety of methods. For example, most data compiled in the “GISS Global Seawater
60 Oxygen-18 Database -V1.21” for stable seawater isotopes (LeGrande and Schmidt, 2006)
61 originate from Isotope-ratio Mass Spectrometry (IRMS). They were mostly measured in



4

62 earlier decades by dual-inlet technology (highest precision), whereas, more recently, the
63 continuous-flow method (lower precision) became widespread for seawater isotope
64 analysis. In the last decade, cavity ring-down spectroscopy (CRDS) turned into another
65 commonly used method as it allows parallel measurement of $\delta^{18}\text{O}$ and $\delta^2\text{H}$, but with
66 often lower precision (e.g., Voelker et al., 2015). Reverdin et al. (2022) recently compiled
67 a mix of data produced by IRMS and CRDS at LOCEAN
68 (<https://www.seanoe.org/data/00600/71186/>). As CRDS and other laser techniques
69 (Glaubke et al., 2024) have become more prevalent recently, they contribute a
70 significant part of the new data produced and thus also to the soon to be released
71 CoralHydro2k seawater database for $\delta^{18}\text{O}$ ($\delta^2\text{H}$) (focus on the tropics (35°N-35°S);
72 Atwood et al., 2024). There are potential differences between the data produced by the
73 two methods. Typically, CO_2 -water or H_2 -water equilibration was used for the IRMS
74 measurements and yields measurements of the activity of water, which decreases with
75 increasing salinity. Furthermore, concentration of divalent cations like Mg^{++} are
76 responsible for slight changes in fractionation factors. On the other hand, the laser
77 methods such as CRDS evaporate the entire sample. If the samples have not been
78 distilled beforehand, there is an issue of salt deposition and of resulting absorption or
79 desorption of water with fractionation effects. In the LOCEAN database (Reverdin et al.,
80 2022), an attempt was made to adjust the data, based on the analysis of Benetti et al
81 (2017b). This was also adopted by at least one other group (Haumann et al., 2022), but
82 overall, there is the possibility of an offset of these data with respect to the ones of other
83 groups using CRDS.

84 It is actually quite common when using water isotope data in studies involving more
85 than one data set, to first evaluate whether there are possible offsets. Intercomparison
86 with earlier data or reference materials was a prerequisite for GEOTRACES sampling
87 campaigns, although for the water isotopes this was, unfortunately, seldomly followed
88 (e.g., Voelker et al., 2015). These intercomparisons often outline systematic differences
89 which could result from the issue outlined above, or from other issues, such as
90 uncertainties in reference materials used, analysis protocols, or isotopic changes in the
91 samples during their handling and storage (Benetti et al., 2017a; Akhoudas et al., 2019;
92 Hennig et al., 2024). In other cases, this was not done, either because the data stood by
93 themselves (Bonne et al., 2019, for $\delta^{18}\text{O}$ and $\delta^2\text{H}$ data), or there was no comparison data



5

94 available in the same region (Glaubke et al., 2024, for $\delta^{18}\text{O}$ data). The possible offsets can
95 however become an issue, when these data are placed in a larger context. For example,
96 Glaubke et al. (2024) identify a large difference in the S- $\delta^{18}\text{O}$ relationship in the
97 subtropical Indian Ocean between their data in the south-eastern part and other data in
98 the south-western Indian Ocean. They also discuss and question differences in the deep
99 water-masses isotopic values between separate data sets, but as these might also be
100 explained by large uncertainties in these data, we will not address them further.

101 Using these two examples (Bonne et al., 2019; Glaubke et al., 2024), the aim of this note
102 is to point out the interest when producing a new data set, of exchanging collected
103 samples to carry a direct comparison, or, if this was not done, to compare the data with
104 other published data and evaluate potential systematic differences.

105 2. Comparisons

106 For identifying possible offsets, we consider surface ocean subsets of the LOCEAN data
107 base in specific regions for roughly the same years as the other data collected. The data
108 extracted are from the same regions as in the datasets of the two studies and are
109 gathered in S- $\delta^{18}\text{O}$ space as well as in S- $\delta^2\text{H}$ space (available only for the Bonne et al
110 (2019) data set), where S is reported as a practical salinity with the practical salinity
111 scale of 1978 (pss). The assumption done here as in many papers is that the S- $\delta^{18}\text{O}$
112 relationship holds on fairly large scales in the surface layer (for the eastern subtropical
113 North Atlantic, see for example, the discussion in Voelker et al (2015) and in Benetti et
114 al. (2017a)). Obviously, this has limitations, such as in areas influenced by more than
115 one water mass or by multiple freshwater end-members (meteoric, continental run-off,
116 sea ice melt or formation, evaporation).

117 2.1 Daily surface data collected from R.V. Polarstern

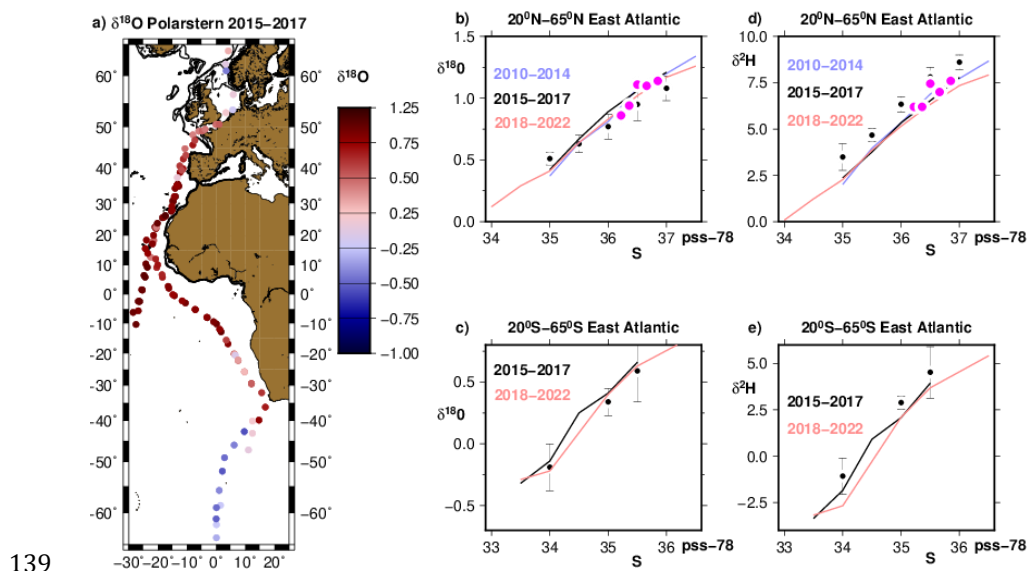
118 The surface seawater samples originated from daily collection during two years on
119 board RV Polarstern in 2015-2017 (Bonne et al., 2019). There is no salinity provided
120 with the data, and here we chose to associate them with the simultaneously collected
121 thermosalinograph (TSG) data collected on board the RV Polarstern and available from
122 PANGAEA (for each cruise, an indexed file with title starting by 'Continuous
123 thermosalinograph oceanography along Polarstern' is included in PANGAEA: for example,



6

124 TSG data for the first cruise (PS90) associated with the isotopic seawater data are found
125 at <https://doi.org/10.1594/PANGAEA.858885>). The water samples were not collected
126 from the same water line and pumping depth as the TSG data, which can result in
127 differences. This is however likely to be small in most circumstances away from large
128 freshwater input at the sea surface, such as from melting sea ice, intense rainfall and
129 river estuaries. We also applied an adjustment of +0.25‰ to the $\delta^{18}\text{O}$ data of Bonne et al.
130 (2019), based on post-analysis identification of a bias in an internal reference material.

131 We then estimate averages of all the data as a function of salinity in two domains
132 extending poleward of the subtropical salinity maximum toward the higher latitudes in
133 the eastern part of the Atlantic Ocean (thus, 20°N to 65°N and the same in the southern
134 hemisphere). This is done by sorting out the data by salinity classes of 0.5. The LOCEAN
135 data until 2016 in the North and tropical Atlantic were presented in Benetti et al
136 (2017a), showing the tightness of the S- $\delta^{18}\text{O}$ and S- $\delta^2\text{H}$ relationships in vast domains of
137 the eastern Atlantic. In the North Atlantic, LOCEAN data have been continuously
138 collected since 2011, and south of 10°S in the eastern Atlantic mostly since 2017.



139

140

141



7

142 Figure 1: Comparison to Bonne et al. (2019). (a) map of RV Polarstern original data set points
143 in eastern Atlantic Ocean east of 30°W. Water isotopes-S scatter diagrams averaged as a
144 function of salinity in 0.5 pss salinity bins (left for $\delta^{18}\text{O}$, and right for $\delta^2\text{H}$), top for the
145 northern hemisphere and bottom for the southern hemisphere, east of 30°W and outside of
146 [20°N, 20°S]. The colored curves represent average relationships of water isotopes in the
147 LOCEAN data base as a function of salinity for three different period ranges, whereas the
148 black dots with error bars are the binned averages of the Bonne et al. (2019) RV Polarstern
149 data in 2015-2017 (after adjustment of +0.25‰ to $\delta^{18}\text{O}$), with the root mean square of the
150 variance reported as error bars. Five individual surface points from Voelker et al (2023) are
151 also plotted (magenta dots).

152 The average relationships found in the LOCEAN data set for three periods overlay well
153 in particular in the northern hemisphere. Uncertainties on individual curves (not
154 shown) are estimated based on the scatter of individual data in each salinity bin. They
155 are typically on the order of 0.01-0.02 (0.05-0.10) ‰ for $\delta^{18}\text{O}$ ($\delta^2\text{H}$) respectively in the
156 northern hemisphere (top panel), and a little larger for the less sampled southern
157 hemisphere curves in 2015-2017. Sampling is usually also insufficient at the low end of
158 the salinity range, to reliably estimate an uncertainty. Thus, these different curves nearly
159 overlay within the sampling uncertainty. Five surface samples that were collected in the
160 Northeast Atlantic during the same years within the same salinity range (Voelker et al.,
161 2023), also fit well on the North Atlantic curves. The adjusted $\delta^{18}\text{O}$ data from Bonne et
162 al. (2019) are slightly shifted downward with respect to the curves (Fig. 1b, c), with the
163 plotted standard deviation of individual data around the average not overlapping the
164 LOCEAN data average curves in most cases for the same years 2015-2017. The situation
165 is opposite for the 35 pss bin in the northern hemisphere, with the adjusted $\delta^{18}\text{O}$ data
166 from Bonne et al. (2019) being above the three LOCEAN average curves, which might be
167 due to samples collected uniquely in the English Channel and North Sea by RV
168 Polarstern in this salinity range, whereas sampling is more geographically-spread in the
169 LOCEAN data base. A difference is also found for $\delta^2\text{H}$, with LOCEAN data been lower than
170 $\delta^2\text{H}$ from Bonne et al. (2019) (Fig. 1d, e).

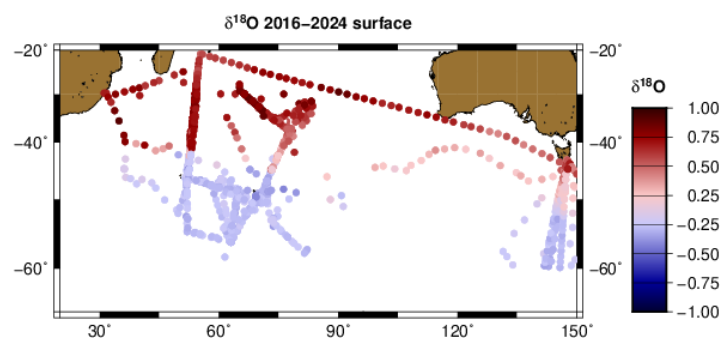
171

172 2.2 Southern subtropical Indian Ocean



8

173 Glaubke et al. (2024) describe a synthesis of water isotope data in the southern Indian
174 Ocean combining their new dataset in the southeastern Indian Ocean (CROCCA-2S) with
175 earlier data in the south-western Indian Ocean, in particular from LOCEAN, as well as
176 data from the south Australian shelf collected mostly in 2010 (Richardson et al., 2019),
177 and in the equatorial Indian Ocean (Kim et al., 2021). In the most recent version of the
178 LOCEAN data set, in addition to data included in Glaubke et al. (2024) for comparison
179 and collected mostly west of 80°E, there are two transects with surface data through the
180 southeastern Indian Ocean, one collected in February 2017, and the other in March
181 2024, thus in mid to late austral summer. These transects cross the region covered by
182 the CROCCA-2S data set, albeit not close to west Australia, as well as the area of the
183 Richardson et al. (2019) data set, south of Australia. The LOCEAN data set also contains
184 surface data south of Tasmania (in 2017, as well as in 2020 to 2024). All these data
185 correspond to samples analyzed on a CRDS Picarro L2130 at LOCEAN, and with the
186 protocols discussed in Reverdin et al. (2022). The bottles in which the samples were
187 stored were the same for all the samples, and time between collection and analysis
188 varied, but was mostly on the order of 6 months or less. Thus, this is a rather
189 homogeneously produced set of data in for the years 2016-2024, which spatially
190 overlaps with the data used in Glaubke et al. (2024) collected south of Australia and in
191 the southeastern Indian Ocean (Fig. 2).



192

193 Figure 2: Map of $\delta^{18}\text{O}$ surface data in the LOCEAN archive for 2016-24, north of 60°S. All
194 these data are associated with S and $\delta^2\text{H}$ data.

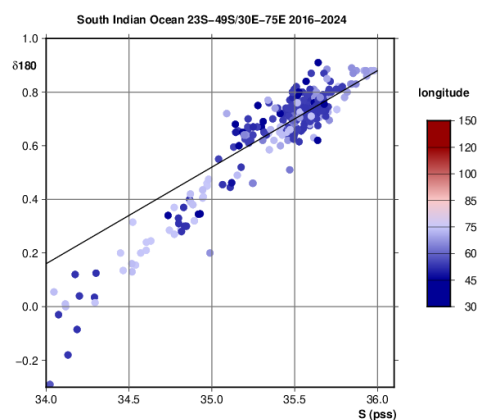
195 The LOCEAN data distribution indicates some scatter in the S- $\delta^{18}\text{O}$ distribution in the
196 southwestern Indian Ocean (Fig. 3a) for S larger than 35 pss. Data above the regression



9

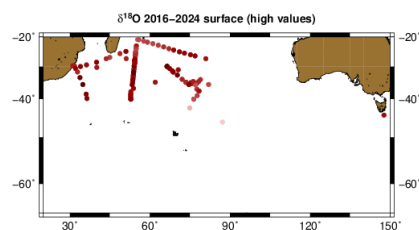
197 line on Fig. 3a, established for all data with S between 35 and 36 pss, are present only for
198 S larger than 35.0 pss, and are found north of 28°S and in the far south-western Indian
199 Ocean, but with some remnants found all the way to the core of the subtropical gyre
200 near 75°E/35°S (Fig. 3b). Data below the regression line contain most of the data south
201 of 28°S and east of 60°E and connect the salinity maximum region with the lower
202 salinity south of the subtropical front and down to the region south of the polar front
203 (Fig. 3c). These subtropical lower values in S- $\delta^{18}\text{O}$ space, which appear in the repeated
204 French OISO cruises (in 1998-2024) at 50°E, albeit not all the time, dominate east of
205 60°E.

206 a)



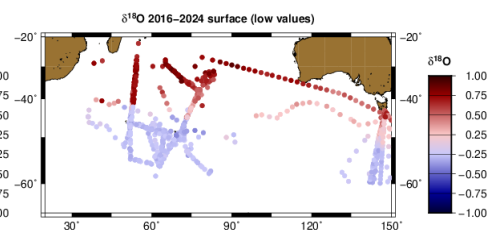
207

208 b)



209

c)



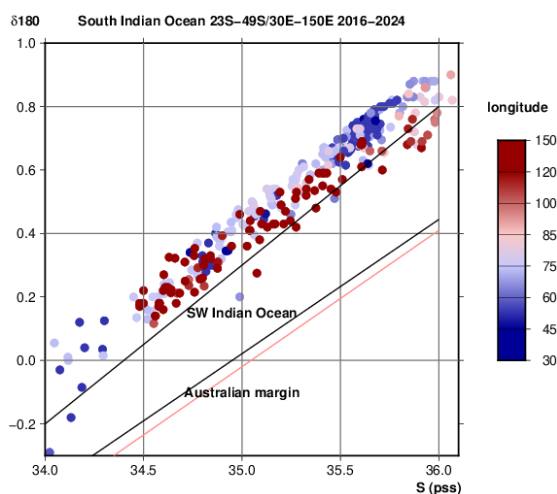
210 Figure 3: (a) scatter diagram of (S, $\delta^{18}\text{O}$) LOCEAN data within the southwestern region (30-
211 75°E/23-49°S) coloured as a function of longitude, with the regression line of the data having
212 a salinity between 35 and 36 pss (black line) overlaid. The spatial distributions of the



10

213 LOCEAN data with higher and lower $\delta^{18}\text{O}$ relative to that regression line in the whole Indian
214 Ocean north of 60°S are shown on panels (b) and (c), respectively.

215 When focusing on the lower part of the distribution in S - $\delta^{18}\text{O}$ space (Fig. 3c), one
216 observes a gradual lowering of $\delta^{18}\text{O}$ from west to east for salinities above 35 (Fig. 4) all
217 the way to 150°E . This lowering is on the order of 0.15 at most, even for the higher
218 salinities (35.5 or more) for which it is strongest (Fig. 4).



219

220 Figure 4: The LOCEAN data below the regression line of Fig. 3a (the ones mapped in Fig. 3c)
221 in S - $\delta^{18}\text{O}$ space, color-coded as a function of longitude. The two linear relationships
222 recommended in this region between 23°S and 49°S by Glaubke et al. (2024) for the south-
223 west Indian Ocean and for the Australian margin (south of Australia) (we use the original
224 $\delta^{18}\text{O} = 0.4231 * S - 14.7876$, instead of the rounded-up relation reported in the paper; R. H.
225 Glaubke, pers. Comm., 2024) are also plotted (black lines), as well as the earlier linear
226 relationship for the 0-600m layer along the Australian margin by Richardson et al. (2018) (in
227 pink).

228 Thus, besides some gradual and smaller changes, we do not observe in the LOCEAN
229 surface dataset a large sudden change in the $(S, \delta^{18}\text{O})$ distribution near 75°E or 85°E
230 between the southeastern and southwestern Indian Ocean, nor a further strong change
231 closer to the Australian coastal margin, as suggested by figures 6 and 7 of Glaubke et al.
232 (2024). Most of the LOCEAN $(S, \delta^{18}\text{O})$ data south of 28°S correspond to the mixing of a



11

233 low salinity end-member characteristic of the fresh waters of the Southern Ocean (at $S <$
234 34 pss) with waters which are imprinted by air-sea exchange of water in a wider range
235 of values at $S > 36$ pss, as discussed in Glaubke et al (2024). These LOCEAN (S , $\delta^{18}O$)
236 values are significantly above the linear relationships proposed by Glaubke et al. (2024),
237 in particular for the Australian coastal margins. Furthermore, the LOCEAN data support
238 the presence of a secondary low salinity end member at $S < 35$ pss with heavier isotopic
239 composition, contributing to the water mass properties in the far southwestern Indian
240 Ocean as well as for the area sampled between $20^{\circ}S$ and $28^{\circ}S$ north of the subtropical
241 salinity maximum. This could be a contribution of the Indonesian Through Flow and
242 tropical western Indian Ocean surface waters, as discussed by Kim et al. (2021) and
243 Glaubke et al. (2024).

244 3. Discussion

245 In the two cases, we find significant differences between the data sets compared. In the
246 case of the RV Polarstern dataset (Bonne et al., 2019), an error in a specified reference
247 material value was found, and the adjusted data present only small offsets with respect
248 to LOCEAN data, that are slightly negative for $\delta^{18}O$ and slightly positive for δ^2H .
249 Differences might arise from spatial differences. For example, in the northern
250 hemisphere, values at salinity close to 35 pss mostly originate from the North Sea and
251 English Channel in the Polarstern dataset, thus with more mid-latitude continental
252 influence than for most of the LOCEAN data in the same salinity range which have a
253 contribution of more depleted subpolar and polar freshwater. One expects a larger
254 scatter in the South Atlantic for salinities less than 35 pss, due to intermittent presence
255 of sea ice or iceberg melt, and at higher salinities due to the presence of different water
256 masses originating from the South Atlantic and southeastern Indian Ocean. However, the
257 current data set is not sufficient to estimate it.

258 Furthermore, different seasons were sampled in the two datasets. In the northeastern
259 Atlantic sector, Bonne et al. (2019) surface data east of $30^{\circ}W$ were collected in in April
260 and November north of $10^{\circ}S$ and in November south of $10^{\circ}S$ in the southeastern
261 Atlantic. These data do not suggest large seasonal differences in the Northeast Atlantic,
262 concurring with the LOCEAN (S , $\delta^{18}O$) data in the tropics to mid-latitudes (20 to $50^{\circ}N$),
263 which are tightly distributed along a mean S - $\delta^{18}O$ relationship, and thus with low



12

264 seasonal variability (Benetti et al., 2017a; Voelker et al., 2015). The LOCEAN data are
265 not numerous enough in the South-East Atlantic to further evaluate whether the offset is
266 constant throughout the data set, or presents a component related to geophysical
267 temporal or spatial variability.

268 When considering the South Indian Ocean, Glaubke et al. (2024) combined data sets that
269 were processed in different institutes, and potential offsets between those could cause
270 the differences in spatial variability. In particular, Glaubke et al. (2024) outline large
271 spatial contrasts in the S- $\delta^{18}\text{O}$ relationship across the surface subtropical Indian Ocean
272 and southern Australia that are not observed in the recent version of the LOCEAN
273 database. Seasonal or interannual variability might also contribute to the differences
274 shown on Fig. 3, as the data in the southeastern Indian Ocean from Glaubke et al. (2024
275 were collected in November-December, whereas the data in the LOCEAN database in
276 this region are mostly from February-March. However, at least south of Tasmania,
277 where the LOCEAN data base also contains December data, it does not seem that the
278 seasonal cycle would cause differences larger than 0.05 ‰ at the same salinity. A
279 difference due to seasonality is thus barely identifiable, noting the possible presence of
280 interannual variability and that 0.05 ‰ is the long-term accuracy in the analyses in
281 some centers, such as AWI Potsdam and LOCEAN. Richardson et al. (2018) also
282 commented that there was little difference between a southern winter cruise and March
283 data south of Australia. Further west, near 55-70°E, earlier surface data in the OISO
284 surveys, as well as the vertical upper profiles of OISO station data also suggest a rather
285 modest seasonal variability on the order of 0.10‰. Changes could also arise from
286 interannual variability, but the range of interannual variability in the LOCEAN data base
287 is smaller than the difference between the Glaubke et al (2024) curves for the
288 southeastern Indian Ocean and south of Australia and the corresponding LOCEAN data.
289 Thus, a likely contribution for the large differences would be the existence of systematic
290 offsets between the South Indian Ocean/Australia margin data produced in three
291 different institutes that were combined in the Glaubke et al. (2024) study.

292 4. Conclusions

293 What these two comparisons suggest is that offsets are present between different recent
294 data sets published, which exceed 0.10‰ in $\delta^{18}\text{O}$ and 0.50‰ in $\delta^2\text{H}$, thus larger than the



295 target long-term accuracy of analyses in individual isotopic laboratories. Moreover,
296 errors in reference material values are always possible and require some post-analysis
297 intercomparisons, such as the one that led to the correction of the RV Polarstern Bonne
298 et al. (2019) data set. Furthermore, one contribution to a systematic difference between
299 the LOCEAN data set and data from other institutes is that the LOCEAN data are
300 reported in concentration scale (Benetti et al., 2017b), thus equivalent to 'freshwater'.
301 The use of the concentration scale corrects possible effects of salt in the water activity
302 measured by IRMS and the effect of salt accumulation during evaporation in laser
303 spectroscopy, which both can lead to fractionation, possibly of similar magnitude
304 (Walker et al., 2016). Different comparisons based on duplicates collected during cruises
305 suggest that this is a main cause of difference between LOCEAN data and other data sets
306 (LOCEAN $\delta^{18}\text{O}$ data been more positive). Poor conservation of the samples during
307 storage, analytical protocols, or uncertainties in the specified values of reference
308 material are other sources of differences between data produced in different institutes.

309 The methods to carry the intercomparisons and detect systematic differences between
310 different data sets are not numerous. On one hand, one could compare values obtained
311 in specific water masses, for which we expect little variability of the water isotopic
312 composition. This is often used, but such data are not always available, and the resulting
313 uncertainties are difficult to assess. One could also develop a method based on the
314 systematic comparison of nearby data, as is suggested in Fig. 1 when comparing the S-
315 water isotopes surface distribution in the North and South Atlantic in the LOCEAN and
316 the RV Polarstern (Bonne et al., 2019) data sets. This could be further improved, but
317 requires that there are enough overlapping data within regions of relatively
318 homogeneous signals. As the data density is not always sufficient, these approaches may
319 fail. Thus, an important alternative approach is to actively share well-preserved water
320 samples, distributed quickly, and dedicated to specific intercomparison of data
321 produced in the different laboratories, building on previous efforts for $\delta^{13}\text{C}$ -DIC (Cheng
322 et al., 2019). This, together with establishing well-accepted systematic guidelines for
323 data production and quality control, and enhancing scientific exchange between the
324 different institutes needs to be actively pursued, in order to reduce the errors when
325 merging different datasets and increase the potential use of the water isotope data as
326 EOVS/ECCVs. Without this effort, the usefulness of the isotopic data for different



14

327 oceanographic and climate studies is strongly reduced, for example resulting in large
328 uncertainties when establishing different S- $\delta^{18}\text{O}$ (or S- $\delta^2\text{H}$) relationships to validate
329 studies of proxies to support paleo-climate reconstructions.

330

331 Data availability

332 The LOCEAN data are available at <https://www.seanoe.org/data/00600/71186/>.

333 The isotopic data of the Bonne et al. (2019) are available as indicated in the paper, with
334 here S added, as described in the text from the PANGAEA archive. The Glaubke et al.
335 (2024) data are available as described in the paper. However, among the data used in
336 this paper, we could not access the data from the Richardson et al. (2019) paper.

337

338 Author contribution: GR initiated the study and prepared the manuscript with
339 contributions from all coauthors. AV initiated the intercomparison effort, and AV, CW,
340 and HM contributed to editing the paper. HM was also responsible from producing the
341 data in the Bonne et al. (2019) paper.

342

343 Competing interests: The authors declare that they have no conflict of interest.

344

345 Acknowledgments

346 The LOCEAN isotopic laboratory is supported by OSU Ecce Terra of Sorbonne Université.
347 We are thankful to Catherine Pierre and Jérôme Demange who have set and help run the
348 facility, such as, and for Aïcha Naamar, Marion Benetti and Camille Akhoudas to have
349 measured some of the water samples. We are grateful for support by INSU for samples
350 during the OISO cruises on RV MD2, and by IPEV during the SOCISSE program on RV
351 Astrolabe, with on board support by Patrice Bretel and Rémi Foletto. A. Voelker thanks J.
352 Waniek (IOW, Germany) for collecting the NE Atlantic water samples and R. van Geldern
353 (GeoZentrum Nordbayern, Germany) for analyzing them. She, also, acknowledges
354 financial support by Fundação para a Ciência e a Tecnologia (FCT) through projects
355 Centro de Ciências do Mar do Algarve (CCMAR) basic funding UIDB/04326/2020
356 (<https://doi.org/10.54499/UIDB/04326/2020>) and programmatic funding
357 UIDP/04326/2020 (<https://doi.org/10.54499/UIDP/04326/2020>) and the CIMAR
358 associated laboratory funding LA/P/0101/2020
359 (<https://doi.org/10.54499/LA/P/0101/2020>). The RV Polarstern data set was funded



15

360 by the AWI Strategy Fund Project ISOARC. Comments by Alexander Haumann were very
361 helpful.

362

363 References

364 Aoki, S., Kobayashi, R., Rintoul, S.R., et al. : Changes in water properties and flow regime on
365 the continental shelf off the Adélie/George V Land coast, East Antarctica, after glacier tongue
366 calving, *J. Geophys. Res.: Oceans*, 122, 6277-6294, 2017.

367 Akhoudas, C. H., Sallée, J.-B., Haumann, F.A., Meredith, M.P., Garabato, A.N., Reverdin,
368 G., Jullion, L., Aloisi, G., Benetti, M., Leng, M.J., and Arrowsmith, C.: Ventilation of the
369 abyss in the Atlantic sector of the Southern Ocean, *Nature scientific reports*, **11**, 16733,
370 <https://doi.org/10.1038/s41598-021-95949-w>, 2020, 2021.

371 Atwood, A. R., Moore, A.L., Long, S., Pauly, R., DeLong, K., Wagner, A., and Hargreaves,
372 J.A.: The CoralHydro2k Seawater $\delta^{18}\text{O}$ Database, *Past Global Changes Magazine* 32,59, doi:
373 10.22498/pages.32.1.59, 2024.

374 Benetti, M., Reverdin, G., Aloisi, G., Sveinbjörnsdóttir, A.: Stable isotopes in surface waters
375 of the Atlantic Ocean: indicators of ocean-atmosphere water fluxes and oceanic mixing
376 processes. *J. Geophys. Res. Oceans*, doi:10.1002/2017JC012712, 2017a.

377 Benetti, M., Sveinbjörnsdóttir, A. E., Ólafsdóttir, R., Leng, M.J., Arrowsmith, C., Debondt,
378 K., Fripiat, F., and Aloisi, G.: Inter-comparison of salt effect correction for $\delta^{18}\text{O}$ and $\delta^2\text{H}$
379 measurements in seawater by CRDS and IRMS using the gas-H₂O equilibration method,
380 *Marine chemistry*, doi:10.1016/j.marchem.2017.05.010, 2017b.

381 Bonne, J.-L., Behrens, M. Meyer, H., Kipfstuhl, S., Rabe, B., Schönicke, L., Steen-Larsen, H.
382 C., Werner, M.: Resolving the controls of water vapour isotopes in the Atlantic sector. *Nature*
383 *Communications* 10, 1632, doi: 10.1038/s41467-019-09242-6, 2017.

384 Brady, E. , Stevenson, S., Bailey, D., Liu, Z., Noone, D., Nusbaumer, J., Otto-Bliesner, B.L.,
385 Tabor, C., Thomas, R., Wong, T., Zhang, J., Zhu, J.:The connected isotopic water cycle in the
386 Community Earth System Model Version 1, *J. Adv. Model. Earth Syst.*, 11, 8,
387 <https://doi.org/10.1029/2019MS001663>, 2019.

388 Cauquoin, A., Werner, M., Lohmann, G.: Water isotopes – climate relationships for the mid-
389 holocene and preindustrial period simulated with an isotope-enabled version of MPI-ESM,
390 *Clim. Past* 15, 1913-1937, <https://doi.org/10.5194/cp-15-1913-2019>, 2019.

391 Cheng, L., Normandeau, C., Bowden, R., Doucett, R., Gallagher, B., Gillikin, D.P.,

392 Kumamoto, Y., McKay, J.L., Middlestead, P., Ninnemann, U., Nothaft, D., Dubinina, E.O.,



16

- 393 Quay, P., Reverdin, G., Shirai, K., Mørkved, P.T., Theiling, B.P., van Geldern, R., and
394 Wallace, D.W.R.: An international intercomparison of stable carbon isotope composition
395 measurements of dissolved inorganic carbon in seawater, *Limnology and Oceanography*:
396 *Methods* 17, 200-209, <https://doi.org/10.1002/lom3.10300>, 2019.
- 397 Glaubke, R. H., Wagner, A., and Sikes, E. L.: Characterizing the stable oxygen isotopic
398 composition of the southeast Indian Ocean, *Marine Chemistry*, 262,
399 <https://doi.org/10.1016/j.marchem.2024.104397>, 2024.
- 400 Haumann, F. A. et al. : [Data set], Zenodo, doi:10.5281/zenodo.1494915, 2019.
- 401 Hennig, A., Mucciarone, D.A., Jacobs, S.S., Mortlock, R.A., and Dunbar, R.B.: Meteoric
402 water and glacial meltwater in the southeastern Amundsen Sea: a time series from 1994 to
403 2020, *The cryosphere*, 18, 791-818, <https://doi.org/10.519/tc-18-791-2024>, 2024.
- 404 Hilaire-Marcel, C., Kim, S.T., Landais, A., Ghosh, P., Assonov, S., Lécuyer, C., Blanchard,
405 M., Meijer, H.A., and Steen-Larsen, H.C.: A stable isotope toolbox for water and inorganic
406 carbon cycle studies, *Nature Reviews Earth & Environment* 2 (10), 699-719, 2021.
- 407 Kim, Y., Rho, T., and Kang, D.-J.: Oxygen isotope composition of seawater and salinity in
408 the western Indian Ocean: Implications for water mass mixing, *Mar. Chem.* 237, 104035,
409 <https://doi.org/10.1016/j.marchem.2021.104035>, 2021.
- 410 Konecky, B.L. et al.: The Iso2k database: a global compilation of paleo- $\delta^{18}\text{O}$ and $\delta^2\text{H}$ records
411 to aid understanding of Common Era climate, *Earth Syst. Sci. Data*, 12, 2261–2288,
412 <https://doi.org/10.5194/essd-12-2261-2020>, 2020.
- 413 Kumar, P.K., Singh, A., and Ramesh, R.: Convective mixing and transport of the Bay of
414 Bengal water stir the $\delta^{18}\text{O}$ -salinity relation in the Arabian Sea., *J. Mar. Sys.* 238, 103842,
415 <https://doi.org/10.1016/j.jmarsys.2022.103842>, 2023.
- 416 LeGrande, A.N. and Schmidt, G.A.: Global gridded data set of the oxygen isotopic
417 composition in seawater, *Geophys. Res. Lett.* 33, <https://doi.org/10.1029/2006gl026011>,
418 2006.
- 419 Oppo, D.W., Schmidt, G.A., and LeGrande, A.N.: Seawater isotope constraints on tropical
420 hydrology during the Holocene, *Geophys. Res. Lett.* 34, L13701,
421 <https://doi.org/10.1029/2007GL030017>, 2007.
- 422 Reverdin et al.: The CISE-LOCEAN sea water isotopic database (1998-2021), *Earth sci. sys.*
423 *data*, <https://doi.org/10.5194/essd-2022-34>, 2022.



- 424 Richardson, L.E., Middleton, J.F., Kyser, T.K., James, N.P., and Opdyke, B.N.: Shallow
425 water masses and their connectivity along the southern Australian continental margin, *Deep*
426 *Sea Res. I, Oceanogr. Res. Pap.* 152, 103083, <http://doi.org/10.1016/j.dsr.2019.103083>, 2019.
- 427 Schmidt, G.A., LeGrande, A.N., and Hoffmann, G.: Water isotope expressions of intrinsic
428 and forced variability in a coupled ocean-atmosphere model, *J. Geophys. Res.* 112, D10103,
429 <https://doi.org/10.1029/2006jd007781>, 2007.
- 430 Voelker, A., Colman, A., Olack, G., Waniek, J.J., and Hodell, D.: Oxygen and hydrogen
431 isotope signatures of Northeast Atlantic water masses, *Deep-Sea Res. II*, 116, 89-106.
432 <https://doi.org/10.1016/j.dsr2.2014.11.006>, 2015. Voelker, A.H.: Seawater oxygen and
433 hydrogen stable isotope data from the upper water column in the North Atlantic Ocean
434 (unpublished data). Interdisciplinary Earth Data Alliance (IEDA),
435 <https://doi.org/10.26022/IEDA/112743>, 2023.
- 436 Walker, S.A., Azetsu-Scott, K., Normandeau, C., Kelly, D.E., Friedrich, R., Newton, R.,
437 Schlosser, P., McKay, J.L. Abdi, W., Kerrigan, E., Craig, S.E., and Wallace, D.W.R.: Oxygen
438 isotope measurement of seawater ($\text{H}_2^{18}\text{O}/\text{H}_2^{16}\text{O}$). A comparison of cavity ring-down
439 spectroscopy (CRDS) and isotope ratio mass spectrometry (IRMS), *Limnol. and*
440 *Oceanography: Methods*, 14, 31-38, <https://doi.org/10.1002/lom3.10067>, 2016.